

## Formation of macroporous gel morphology by phase separation in the silica sol-gel system containing nonionic surfactant

Junsheng Wu, Xiaogang Li, Wei Du, and Hua Chen

Materials Science and Engineering School, University of Science and Technology Beijing, Beijing 100083, China

(Received 2004-12-20)

**Abstract:** The phase separation and gel formation behavior in an alkoxy-derived silica sol-gel system containing  $C_{16}EO_{15}$  has been investigated. Various gel morphologies similar to other sol-gel systems containing organic additives were obtained by changing the preparation conditions. Micrometer-range interconnected porous gels were obtained by freezing transitional structures of phase separation in the sol-gel process. The dependence of the resulting gel morphology on several important reaction parameters such as the starting composition, reaction temperature and acid catalyst concentration was studied in detail. The experimental results indicate that the gel morphology is mainly determined by the time relation between the onset of phase separation and gel formation.

**Key words:** silica sol-gel; phase separation; macroporous gel morphology; nonionic surfactant

### 1 Introduction

The sol-gel process is generally recognized to be a promising route for preparing the materials based on metal oxides such as glasses, ceramics, support materials, and even inorganic-organic composites and hybrids [1-2]. Especially, this liquid-phase synthesis method attracts much interest as a process for preparing well-designed porous materials [3],

Silica gels derived from the sol-gel process are essentially porous materials and their structure alters greatly depending on the preparation conditions. Recently, reaction control of the sol-gel process by adding organic compounds has been reported for the purpose of obtaining controlled porous materials. A novel sol-gel process to fabricate well-defined macroporous monoliths has been established based on the polymerization-induced phase separation in various silica-based sol-gel systems including polymer-silica-solvent, surfactant-silica-solvent, and silica-polar solvent systems by Nakanishi and co-workers [4]. By controlling the sol-gel process and post-gelation treatments [5], the silica monoliths usually have a structure of bimodal pores in a discrete size-range of micrometers and nanometers. Such materials have wide applications such as separation media and catalyst supports, because the macropores provide pathways for rapid molecular transportation, and the mesopores create a large area of active surface.

Among the various organic additives which can induce the phase separation in the above silica-based

sol-gel systems, poly(ethylene oxide) and nonionic surfactants containing polyoxyethylene units are useful in that the pore size and pore volume can be controlled more independently [3-4]. Polyoxyethylene alkyl ethers are a group of attractive nonionic surfactants widely used to synthesize mesoporous materials acting as structure-directing agents [6-8]. Thus, it is assumed that self-organized structures of surfactants will template mesopores within the interconnected macroporous framework in these alkoxy-derived sol-gel systems incorporated with nonionic surfactants. The formation of double pore structures in alkoxy-derived silica incorporated with the nonionic surfactant polyoxyethylene nonylphenylether has been reported by Nakanishi *et al.* [3, 9].

Alkyl (ethylene oxide) nonionic surfactants, polyoxyethylene cetyl ethers ( $C_{16}EO_m$ ), are commonly used as templating agents for synthesizing mesoporous materials [7-8]. These were chosen in the present study as organic additives to the sol-gel transition process to induce phase separation. We have investigated in detail the effects of the compositional parameters, acid catalyst concentration, and reaction temperature on the gel morphology, focusing mainly on the phase separation and gelation behavior in an alkoxy-derived silica sol-gel system containing the nonionic surfactant  $C_{16}EO_{15}$ .

### 2 Experimental

Tetramethoxysilane (TMOS, obtained from Wuhan

University Silicone New Material Co. Ltd., China), was used as a silica source. Polyoxyethylene cetyl ether containing 15 oxyethylene units, denoted as C<sub>16</sub>EO<sub>15</sub> (a product of Jiangsu Feixiang Chemical Co., Ltd., China) was used as a nonionic surfactant to induce phase separation. Nitric acid was used as a catalyst for the hydrolysis and polycondensation of alkoxide.

The typical silica monoliths samples were prepared as follows. First, an appropriate amount of surfactant C<sub>16</sub>EO<sub>15</sub> was dissolved in nitric acid aqueous solution of specific concentration and stirred until the surfactant was completely dissolved. Second, TMOS was added to the clear surfactant solution while stirring strongly at room temperature. After stirring for several minutes, the resultant homogeneous and transparent solution was transferred into a plastic container with its top tightly sealed, and then kept at a constant temperature for gelation and aged at the same temperature for 1 to 2 days. Finally, the aged gels were dried at 40°C in a vacuum drying oven for several days.

The morphology of the sample gels was examined with a scanning electron microscope (SEM). The thickness of the dried gel skeleton and the diameter of adjacent pores were measured directly on the SEM photographs and the values reported here were obtained by taking more than 20 measurements and averaging the results.

### 3 Results

#### 3.1 Gelation behavior and gel morphology

Under strongly acidic conditions, after the final addition of TMOS, a homogeneous solution could be obtained within a few seconds under vigorous stirring and the gelation behavior of transparent sols obtained from this was almost the same as that in the previously reported systems containing TMOS [4-9]. The gelation time was greatly influenced by the reaction conditions compared with that in silica sol-gel systems without organic additives. Sudden appearance of turbidity, which implied the onset of phase separation, was observed either before or after gelation in various reaction conditions. Under some conditions, such as water-rich composition, and low acid catalyst concentration, a polymerizing solution became turbid much earlier than gelation, followed by the precipitation of a dispersed phase, and finally giving a distinct two-phase appearance. The gelation time, denoted as  $t_g$ , was determined by simply tilting the container and observing the time at which the bulk fluidity of the sol was lost; and the phase separation time,  $t_{ps}$ , was obtained according to the time at which the sol became

turbid.

In the present experimental system, various morphologies of the resultant gels were formed due to the occurrence of phase separation during the polycondensation reaction of hydrolyzed alkoxysilane, similar to that in other systems reported by Nakanishi and co-workers [9, 11-12]. From the SEM photographs, the structures of gels in the present system were found to contain four typical morphologies, based on the characteristic size and continuity of pores and gel skeletons. These were a homogeneous gel, an interconnected structure, aggregates of particles, and a macroscopic two-phase gel. These various transient structures of phase separation could be frozen-in as a permanent gel morphology, depending on the time relation between the onset of phase separation and gel formation, which described as follows.

(a) In the course of sol-gel transition, in case no symptom of phase separation such as opacification of the solution was observed until gel formation occurred, *i.e.*,  $t_g \ll t_{ps}$ , homogenous gels were formed, which usually appeared transparent or translucent, with a pore size within the nanometer range.

(b) The interconnected structure was observed when the transitional phase separation structure freezing by gel formation almost coincided, *i.e.*,  $t_g \approx t_{ps}$ . In this case the silica skeletons and pores were cocontinuous, and the pore size was in the micrometer range. The aggregates of particles resulted from a relatively early onset of phase separation relative to the gel formation.

(c) When phase separation took place much earlier than gelation, *i.e.*,  $t_g \gg t_{ps}$ , the solution separated macroscopically into two phases, the precipitated phase in the bottom and supernatant phase, because of the difference in density. The silica-rich phase contained isolated pores in its condensed silica matrix (the SEM photographs not showed in the text).

#### 3.2 Dependence of gel morphology on reaction conditions

The gelation time  $t_g$ , phase separation time  $t_{ps}$  and the final gel morphology were greatly influenced by compositional parameters, acid catalyst concentration, and reaction temperature.

**Figure 1** shows the dependence of gelation time,  $t_g$  and phase separation time,  $t_{ps}$  on an incorporated amount of C<sub>16</sub>EO<sub>15</sub>. At the same time, the resultant morphology is also denoted in each data point. The additive amount of C<sub>16</sub>EO<sub>15</sub>, C<sub>C16EO15</sub>, is expressed as a molar ratio of C<sub>16</sub>EO<sub>15</sub> to SiO<sub>2</sub>. In addition, the peri-

odic domain size  $L$ , which is defined as half of the sum of thickness of the gel skeleton and diameter of an adjacent pore [10], is plotted against the surfactant amount only at which the interconnected structure was obtained. **Figure 2** shows the dependence of gelation time, phase separation time, and average domain size on the additive amount of  $H_2O$ , which is expressed as a molar ratio of  $H_2O$  to  $SiO_2$ .

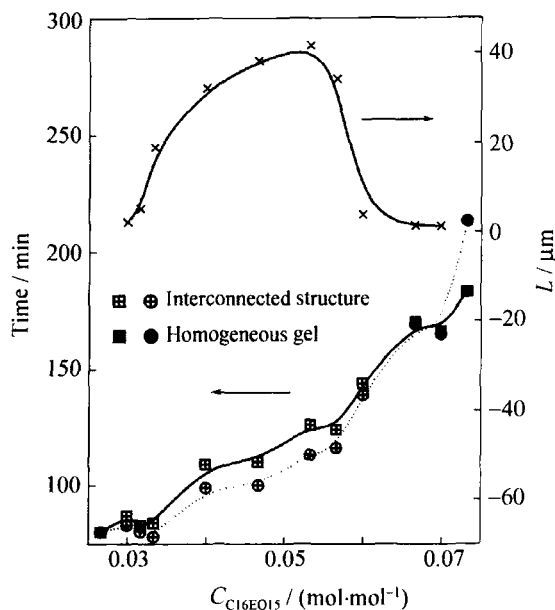


**Figure 1** Dependence of the gelation time ( $t_g$ , square), phase separation time ( $t_{ps}$ , circle), and average domain size ( $L$ , cross) on the additive amount of  $C_{16}EO_{15}$ . The reaction temperature is  $40^\circ C$  and the starting composition is:  $H_2O$  (1 mol/L  $HNO_3$ ), 27.00 g; TMOS, 12.67 g.

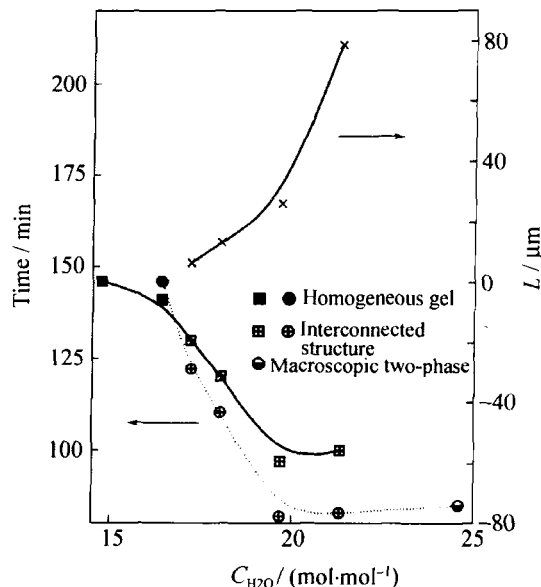


**Figure 2** Dependence of the gelation time ( $t_g$ , square), phase separation time ( $t_{ps}$ , circle), and average domain size ( $L$ , cross) on the additive amount of  $H_2O$ . The reaction temperature is  $40^\circ C$  and the starting composition is: TMOS, 12.67 g;  $C_{16}EO_{15}$ , 3.70 g.

**Figure 3** shows the relation between the starting solution composition and resultant gel morphology for a system containing  $C_{16}EO_{15}$  at  $40^\circ C$ . In the composition triangle, a limited composition region (denoted with a shade area in figure 3) of the co-continuous morphology is recognized where the phase separation and the sol-gel transition parallels to each other.

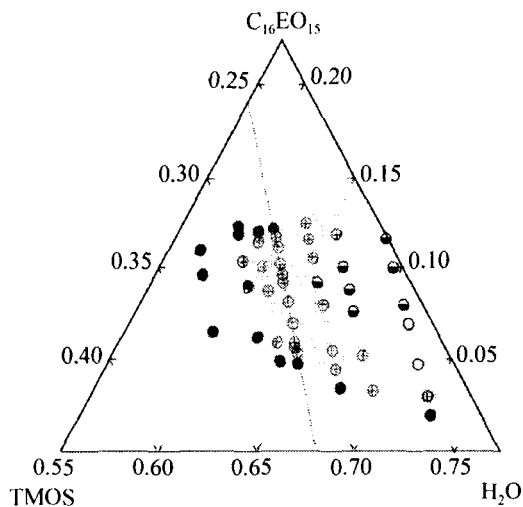


**Figure 3** Dependence of the resultant gel morphology against the starting composition.  $\oplus$ : interconnected structure;  $\bullet$ : homogeneous gel;  $\circ$ : particle aggregates;  $\ominus$ : macroscopic two-phase gel.

Among the compositional parameters, the ratio of  $C_{16}EO_{15}$  to silica has obvious influence on the phase tendency so as to determine the resultant gel structure. **Figure 4** shows the typical morphology of dried gels prepared with different additive amounts of  $C_{16}EO_{15}$  (expressed as a molar ratio of  $C_{16}EO_{15}$  to  $SiO_2$ ) in the starting composition along the dot line in the composition triangle (figure 3).

**Figure 5** shows the dependence of the gelation time  $t_g$ , phase separation time  $t_{ps}$ , average domain size  $L$ , and the gel morphology on the reaction temperature. The experimental results show that in the range of present experiment starting composition, the interconnected structure could not be obtained when the gelation temperature below  $25^\circ C$ , because of the slower polymerization rate of silica oligomers. But when the temperature rising above  $80^\circ C$ , the polymerization rate was too fast to obtain the interconnected structure since the phase separation could not be induced.

**Figure 6** shows that the values of  $t_g$ ,  $t_{ps}$ , and  $L$  depend on the concentration of acid catalyst in solvent water. When the acid catalyst concentration of the solvent becomes lower than  $0.75$  mol-L $^{-1}$ , only the macroscopic two-phase gel can be obtained at  $40^\circ C$ . However, the particle precipitation appears quickly after dropping TMOS into the solution while pH close to the neutral value.

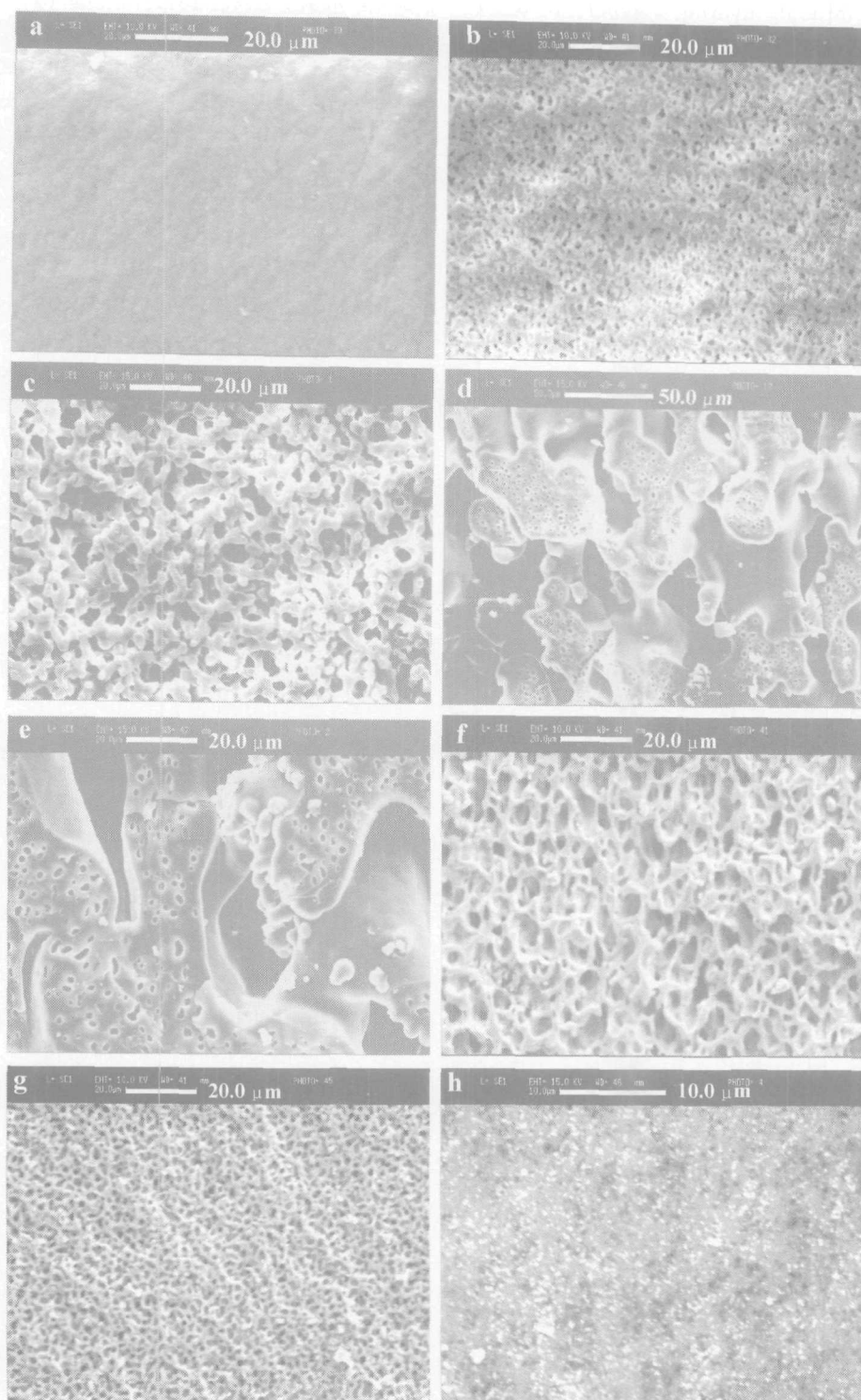


**Figure 4** SEM photographs of dried gel morphology of the samples in the  $C_{16}EO_{15}$ -TMOS system with varied additive amounts of nonionic surfactant: (a)  $C=0.0266$ ; (b)  $C=0.0299$ ; (c)  $C=0.0317$ ; (d)  $C=0.0466$ ; (e)  $C=0.0565$ ; (f)  $C=0.0599$ ; (g)  $C=0.0698$ ; (h)  $C=0.0732$ . The reaction temperature is  $40^{\circ}\text{C}$  and the starting composition is  $\text{H}_2\text{O}$  (1 mol/L  $\text{HNO}_3$ ), 27.00 g; TMOS, 12.67 g.

## 4 Discussion

### 4.1 Mechanism of gel morphology formation

In the present experimental system, the reacting solution contains alkoxy-derived silica, surfactant, catalyst, and solvent, which includes water and methanol produced in the process of hydrolysis and

condensation of TMOS. The nonionic surfactant  $C_{16}H_{33}(OCH_2CH_2)_{15}OH$  ( $C_{16}EO_{15}$ ) exhibits amphiphilic character, constructed by hydrophobic alkyl chain with hydrophilic polyoxyethylene unit. In the course of sol-gel reaction, with the increasing of the polymerization degree of silica oligomers, more surfactant molecules can adsorb onto the polymerizing

silica oligomers through hydrogen bonds between polyoxyethylene chains and surface silanols. Moreover,

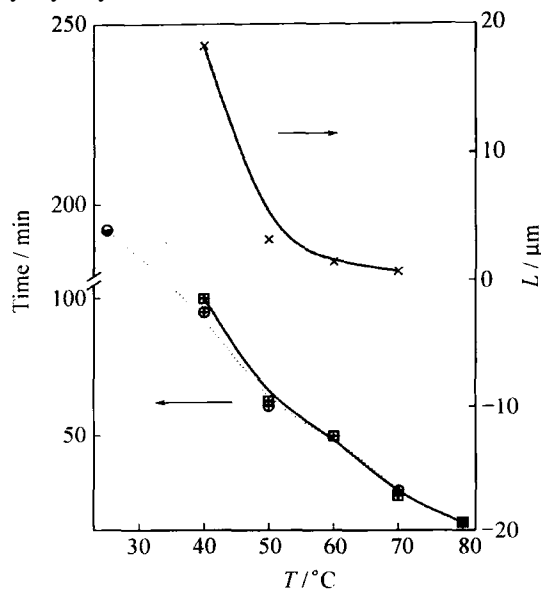


Figure 5 Dependence of the gelation time, ( $t_g$ , square), phase separation time, ( $t_{ps}$ , circle), and average domain size, ( $L$ , cross) on the reaction temperature ( $T$ ). The starting composition is  $\text{H}_2\text{O}$  (1mol / L  $\text{HNO}_3$ ), 27.00 g; TMOS, 12.67 g;  $\text{C}_{16}\text{EO}_{15}$ , 3.45 g. Symbols are the same as in figure 1.

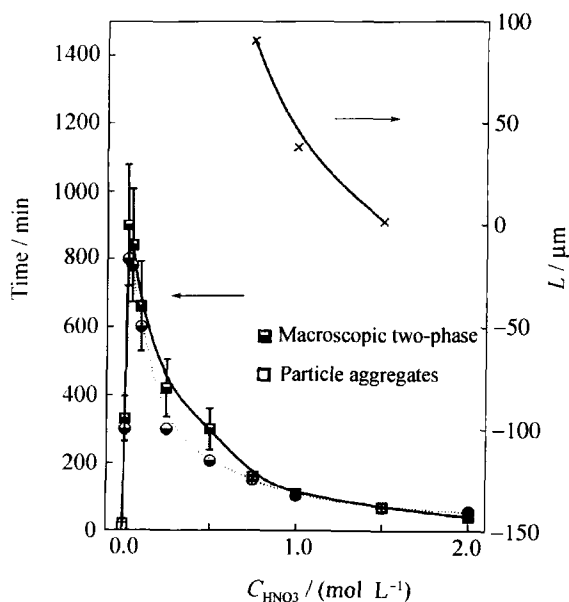


Figure 6 Dependence of the gelation time ( $t_g$ , square), phase separation time ( $t_{ps}$ , circle) and average domain size ( $L$ , cross) on the acid catalyst concentration  $C_{\text{HNO}_3}$ . The reaction temperature is 40°C and the starting composition is:  $\text{H}_2\text{O}$ , 27.00 g; TMOS, 12.67 g;  $\text{C}_{16}\text{EO}_{15}$ , 3.50 g.

ver, the hydrophobicity of outward alkyl chains makes the silica oligomers less soluble in the solvent, and as a result, the system separates into two phases, one rich in solvent and the other rich in surfactant  $\text{C}_{16}\text{EO}_{15}$  and silica. Therefore, this system can be regarded as a quasi binary system. Thus, for the system containing surfactant, the origin of phase separation is assumed to

be the increased repulsive interaction of hydrophobic surface of silica oligomers adsorbed  $\text{C}_{16}\text{EO}_{15}$  molecules against the solvent mixture. Phase separation in this system can be initiated by quench mode of "chemical cooling" (or "chemical quench"), the rise of binodal and spinodal lines due to the polymerization of silica oligomers together with the adsorption of  $\text{C}_{16}\text{EO}_{15}$  molecules, which thrusts a single-phase mixture into a two-phase region (see figure 7). In this process, the compatibility between polymerized silica and solvent becomes lower and lower with the increasing of the polymerization degree of silica oligomers, *i.e.*, the increasing of the molecular weight of polymerized silica,  $N$ . The driving force of phase separation arises when  $N$  exceeds a certain threshold value,  $N_b$ , at which the starting composition is crossed by the equilibrium binodal line [13]. Therefore, when the starting single phase system thrusts into the thermodynamically unstable two-phase region, *i.e.*, the spot 5 of the starting composition within the spinodal line in the phase diagram, the spinodal decomposition can take place (figure 7).

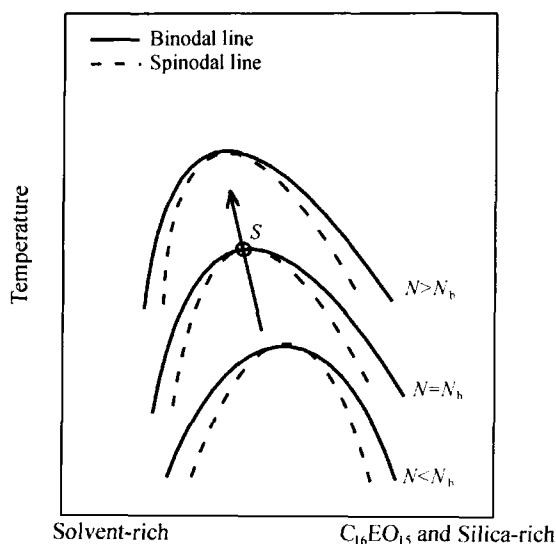
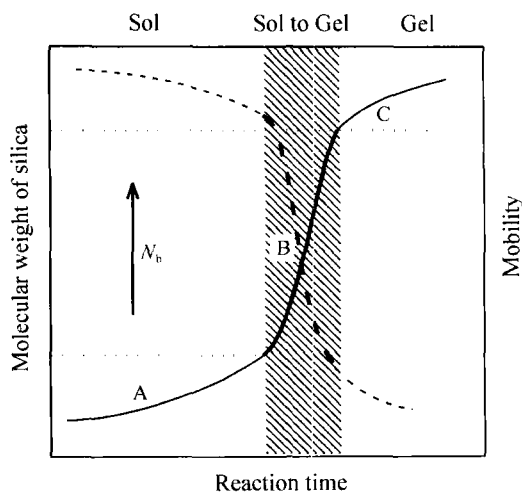


Figure 7 Schematic phase diagram of the quasi binary polymerizing system containing solvent and  $\text{C}_{16}\text{EO}_{15}$ -silica complexes. The spot  $S$  indicates the starting composition and  $N$  denotes the molecular weight of silica.

It is well known that the domain formation induced by spinodal phase separation includes successive three stages, such as initial stage, intermediate stage, and late stage [14]. From the morphological point of view, the intermediate and late stages are regarded as the coarsening process in which the characteristic size of the cocontinuous structure changes from short to longer length scale with time. On the other hand, in the gel forming polymerization reaction, the solution loses its fluidity because of the gel network formation as the molecular weight of polymerized silica,  $N$ , exceeds a

certain value range for gelation,  $N_g$  [13]. When the sol-gel transition occurs concurrently with the structure development by the spinodal separation, the transient structure can be frozen-in in various stages. Therefore, various transient structures of phase separation can be frozen-in as a permanent gel morphology depending on the time relation between the onset of phase separation and gel formation. These situations can be explained in terms of the relation between the above threshold values of molecular weight,  $N_b$  and  $N_g$  [13] (see **Figure 8**).



**Figure 8** Schematic time evolution of the molecular weight of silica (solid line) together with the mobility of the system (dash line) and the relation between  $N_b$  and  $N_g$ .

(1)  $N_b \ll N_g$ . As expressed in region A of figure 8, this situation implies that the compatibility among the polymerized silica adsorbed  $C_{16}EO_{15}$  molecules and solvent mixture is greatly increasing with the polymerization of silica oligomers, and as a result, the molecular weight of polymerized silica is much lower than  $N_g$ , the value range of molecular weight for gelation in the shaded area of figure 8, when the binodal line crosses the starting composition. Thus, phase separation initiates long before the gel formation, *i.e.*,  $t_g \gg t_{ps}$ , discussed ahead. In this case, the phase separation is initiated at shallower quench depth due to the lower viscosity and lower rate of chemical cooling (the binodal line moves slowly), so the phase separation maybe occurs by the nucleation-growth (NG) mechanism. Subsequent sedimentation of  $C_{16}EO_{15}$  and silica-rich phase leads the solution to macroscopic two-phase separation.

(2)  $N_b \cong N_g$ . In region B of figure 8, phase separation is parallel to the formation of the gel network of silica, *i.e.*,  $t_g \cong t_{ps}$ . Due to a steeply increasing of viscosity, a time-consuming NG is suppressed and spinodal phase separation dominates. Because the molecular weight increases steeply with time in the sol-gel region, and the corresponding motion of the binodal

line is accelerated, so the phase separation is initiated at a deeper quench depth, which leads to a shorter periodic wavelength [13]. In this case, the coarsening process of the domains can proceed before they are frozen-in. When the phase separation occurs earlier than gel formation, *i.e.*,  $N_b$  corresponds to the lower value range of  $N_g$ , phase separation proceeds parallel to loose network formation, under which condition a relative prolonged coarsening process can lead to the fragmentation of the phase domains, as a result, the structure of particle aggregates or isolated macropores can be formed. On the other hand, when the phase separation initiates in the later stage of gel formation, *i.e.*,  $N_b$  corresponds to the larger value range of  $N_g$ , the periodic structure with a much shorter wavelength develops in a tightly cross-linked silica network. The domain coarsening can hardly proceed in the rigid network, result in very fine periodic structure even homogeneous dispersed micropores formation. Between these two extremes, the interconnected structure with a wide range of periodic size is obtained when an onset of the phase separation and structure freezing by gel formation almost coincide with each other.

(3)  $N_b \gg N_g$  ( $t_g \ll t_{ps}$ ). In region C, it is implied that the affinity of polymerized silica against solvent mixture can not decrease to enough lower to induce phase separation before gelation, *i.e.*, the binodal line can not reach the position of starting composition before gel formation. The spinodal phase separation may take place in an already cross-linked network. But the coarsening process of domain can not proceed since it requires substantial network mobility. The size of phase-separated domains will be in the nanometer range, and the morphology of the gels becomes almost indistinguishable from that of surfactant-free gels.

## 4.2 Effect of compositional parameters on gel morphology

(1) Dependence of gel morphology on the amount of  $C_{16}EO_{15}$  addition.

As shown in figure 1, the gelation time and phase separation time both monotonously increase with the increase of the incorporated  $C_{16}EO_{15}$  amount. This is probably due to the polymerization of silica oligomers hindered by the surfactant molecules adsorbed onto its surface, *i.e.*, the polymerization rate is decelerated by the adsorption of  $C_{16}EO_{15}$  and the gelation and phase separation are both retarded with the increasing number of adsorbed  $C_{16}EO_{15}$  molecules. As discussed above, the domain size mainly depends on the time relation between the onset of phase separation and gel formation. From figure 1, the value of  $L$  initially increases and then decreases through a maximum (see SEM photographs shown in figure 4), which is in

good agreement with the time relation between  $t_g$  and  $t_{ps}$ . At a lower  $C_{16}EO_{15}$  amount,  $N_b$  can reach a larger value range of  $N_g$  in the later gelation process due to a less number of surfactant molecules adsorbed on the silica oligomers, *i.e.*, the phase separation tendency is relative low since the weak repulsive interaction between the polymerized silica and solvent mixture. Thus the onset of phase separation and structure frozen-in by gel formation almost coincide with each other, and the fine domain of interconnected structure is obtained. With the increase of the number of  $C_{16}EO_{15}$  molecules adsorbed, phase separation tendency is increasing because the surface of polymerized silica becomes more and more hydrophobic against the hydrophilic external solvent. In this case,  $N_b$  is corresponding to the earlier stage value of  $N_g$ , and there is a longer time for the coarsening process before the gel formation than the former situation. When reaching to

the saturated amount of monolayer adsorption, phase separation tendency also reaches to the maximum, *i.e.*, the time gap between  $t_g$  and  $t_{ps}$  gets up to the maximum, and simultaneously the domain size  $L$  achieves its top value. Then, with continuous increasing of the additive amount, there are not enough free spots on silica surfaces for the adsorption of  $C_{16}EO_{15}$  molecules, eventually the second layer adsorption takes place through head to head interaction between the hydrophobic alkyl chains of  $C_{16}EO_{15}$  molecules, which decreases the hydrophobicity of silica surfaces due to the hydrophilic headgroup outward. As a result, the phase separation tendency becomes weaker again, and the time gap between  $t_g$  and  $t_{ps}$  becomes smaller and smaller, which leading to the decrease of the domain size  $L$  again [9]. The overall situation above can be illustrated in **figure 9**.

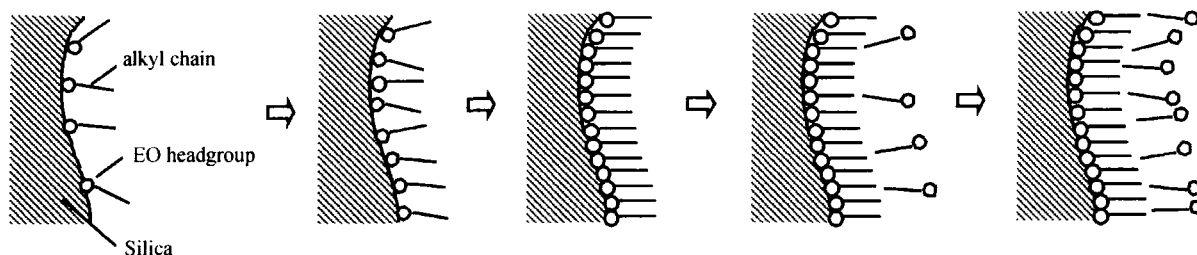


**Figure 9** Schematic representation of the proposed adsorption situation at various added amounts of  $C_{16}EO_{15}$  molecules.

(2) Dependence of gel morphology on the additive amount of water.

According to figure 2, the gelation time and phase separation time both gradually decrease with the increase of the added water concentration. However, the domain size  $L$  monotonously increases with the increase of the amount of water. This change is also well illustrated by the onset of phase separation relative to the gelation as shown in figure 2.

In the present system with abundant water under a strong acid condition, it is assumed that all TMOS molecules in the starting composition are fully hydrolyzed and subsequently polycondensed in the sol-gel reaction, which corresponds to the consumption of 2 mol of water and the generation of 4 mol of methanol per unit mol of TMOS. It was reported that the existence of alcohols generally tends to disturb the adsorption reaction in an aqueous solution [12]. From this viewpoint, at a low additive amount of water, there is a relative abundant methanol rising in the aqueous solution, which will hinder the adsorption of surfactant molecules onto the silica and decrease the phase separation tendency, as a result, the earlier stage structure of phase separation is frozen-in by gel formation. With increasing the amount of added water, the disturbing effect is expected to decrease for the

decrease of methanol concentration. So the phase separation tendency gradually rises and the onset of phase separation tends to occur earlier, as a result, a coarser domain size is obtained. Finally, when the amount of water becomes large enough, the macroscopic two-phase in bottom is observed due to the much earlier occurrence of phase separation and subsequent sedimentation of the polymerized silica.

#### 4.3 Effect of temperature

As shown in figure 5, the gelation and phase separation time both steeply decrease with the increasing of the reaction temperature. This is because that the increased temperature can accelerate both hydrolysis and polycondensation of alkoxy silane. The adsorption of surfactant molecules on the surfaces of silica is an exothermic reaction, thus, the phase separation tendency decreases along with the increase of the reaction temperature due to the adsorption being hindered by thermal disturbance. In this case,  $N_b$  increases to approach and pass through  $N_g$  with increasing the reaction temperature, this coincides with the fact that  $t_{ps}$  gradually approaches and finally surpasses  $t_g$ , and corresponding to the monotonously decreasing of  $L$  as shown in figure 5. The accelerated polymerization denotes the higher chemical cooling rate, *i.e.*, the rapidly moving of binodal line in figure 7, resulting in the

phase separation initiated at a deeper quench depth, which leads to the finer domains. Therefore, with the increase of the reaction temperature, the domain size  $L$  steeply decreases due to the delayed onset of phase separation and accelerated polymerization, which can suppress the prolonged coarsening process of phase domains.

#### 4.4 Effect of acid catalyst concentration

As shown in figure 6, with the increase of nitric acid concentration,  $t_{ps}$  first increases and then decreases steeply through a maximum, at which the pH value of the solution is close to the isoelectric point (IEP) of silica (pH=1.5-2.0) [1]. Although it is difficult to exactly determine the gelation time of highly viscous precipitated phase, the change tendency of  $t_g$  against the acid concentration is similar to  $t_{sp}$ . It is well known that the polymerization rate can be accelerated by increasing the concentration of hydronium ions in the solution when the pH value bellows the IEP of silica. But the phase separation tendency is little influenced by the change of the pH value. In this case, the phase separation can also be initiated at a deeper quench depth at low pH values due to the higher chemical cooling rate and a steeply increasing viscosity of the solution, and the rapid gelation can freeze the finer domain in the earlier stage of the coarsening process. With the increase of the pH value, the decreased polymerization rate results in a shallower quench depth, at the same time, the original periodic structure will experience a longer coarsening process before being frozen-in by gelation because the slow change of viscosity, which leads to coarser domain sizes. Finally, when the onset of the phase separation becomes much earlier than gelation with the increasing of the pH value, the solution can separate macroscopically into two phases because of the much lower viscosity.

## 5 Conclusions

Micrometer range interconnected structures were also formed in the alkoxy-derived silica sol-gel system incorporated with the nonionic surfactant  $C_{16}EO_{15}$ . This system could be regarded as a quasi binary system in the sol-gel process, and the well-defined macropores were presumably formed by freezing transitional structures of spinodal decomposition by gelation. The resultant gel morphologies could be controlled by adjusting the starting compositional parameters, reaction temperature and acid catalyst concentration. The distribution of macropore size from 0.5 to 100  $\mu\text{m}$  was obtained by changing the preparation conditions. The change in pore sizes and gel morphologies could be explained consistently in terms of the competition of the structure development by phase

separation and the structure frozen-in by gel network formation.

## Acknowledgements

The financial support of the present work from the PetroChina Co. Ltd. for scientific research and technology development is gratefully acknowledged.

## References

- [1] J.D. Wright and N.A.J.M. Sommerdijk, *Sol-Gel Materials: Chemistry and Applications*, Gordon and Breach Science Publishers, Amsterdam, 2001, p.85.
- [2] J.Z. Gao, Y.C. Zhao, W. Yang, *et al.*, Sol-gel preparation and characterization of  $\text{Co}_3\text{O}_4$  nanocrystals, *J. Univ. Sci. Technol. Beijing*, 10(2003), No.1, p.54.
- [3] K. Nakanishi, R. Takahashi, T. Nagakane, *et al.*, Formation of hierarchical pore structure in silica gel, *J. Sol Gel Sci. Technol.*, 17(2000), No.3, p. 191.
- [4] K. Nakanishi, Pore structure control of silica gels based on phase separation, *J. Porous Mater.*, 4(1997), No.2, p.67.
- [5] R. Takahashi, K. Nakanishi, and N. Soga, Small-angle X-ray scattering study of nanopore evolution of macroporous silica gel by solvent exchange, *Faraday Discuss.*, 101(1995), p.249.
- [6] S.A. Bagshaw, E. Prouzet, and T.J. Pinna, Templating of mesoporous molecular sieves by nonionic polyethylene oxide surfactants, *Science*, 269(1995), p.1242.
- [7] D. Zhao, Q. Huo, J. Feng, B.F. Chmelka, *et al.*, Nonionic triblock and star diblock copolymer and oligomeric surfactant syntheses of highly ordered, hydrothermally stable, mesoporous silica structures, *J. Am. Chem. Soc.*, 120(1998), No.24, p.6024.
- [8] A. Leonard, J.L. Blin, M. Robert, PA. Jacobs, *et al.*, Toward a better control of internal structure and external morphology of mesoporous silicas synthesized using a nonionic surfactant, *Langmuir*, 19(2003), No. 13, p.5484.
- [9] K. Nakanishi, T. Nagakane, and N. Soga, Designing double pore structure in alkoxy-derived silica incorporated with nonionic surfactant, *J. Porous Mater.*, 5(1998), No.2, p. 103.
- [10] H. Nishino, R. Takahashi, S. Sato, T. Sodesawa, Phase separation in the solution of water glass and poly(vinyl alcohol), *J. Non Cryst. Solids*, 333(2004), No.3, p.284.
- [11] H. Kaji, K. Nakanishi, and N. Soga, Polymerization-induced phase separation in silica sol-gel systems containing formamide, *J. Sol Gel Sci. Technol.*, 1(1993), p.35.
- [12] K. Nakanishi, H. Komura, and R. Takahashi, Phase separation in silica sol-gel system containing poly(ethylene oxide), I. Phase relation and gel morphology, *Bull. Chem. Soc. Jpn.*, 67(1994), No.5, p. 1327.
- [13] K. Nakanishi and N. Soga, Phase separation in gelling silica-organic polymer solution: systems containing poly(sodium styrenesulfonate), *J. Am. Ceram. Soc.*, 74(1991), No.10, p.2518.
- [14] T. Hashimoto, M. Itakura, and H. Hasegawa, Late stage spinodal decomposition of a binary polymer mixture, I. Critical test of dynamical scaling on scattering function, *J. Chem. Phys.*, 85(1986), p.6118.